Pergamon

Cement and Concrete Research 29 (1999) 577–584

CEMENT AND CONCRETE RESEARCH

Hydration kinetics, change of relative humidity, and autogenous shrinkage of ultra-high-strength concrete

Ahmed Loukili [a,*], Abdelhafid Khelidj [b], Pierre Richard [c]

[a]*Laboratoire Génie Civil de Nantes–Saint-Nazaire, Ecole Centrale de Nantes, BP 92101, 44321 Nantes cedex 3, France*
[b]*IUT, BP 420, 44606 Saint-Nazaire, France*
[c]*Direction Scientifique, Bouygues, 78061 St. Quentin en Yvelines, France*

Manuscript received 12 November 1998; accepted manuscript 1 February 1999

Abstract

This research forms part of a vast experimental program designed to investigate the shrinkage and creep of compact reinforced composite (CRC), which is an ultra-high-strength concrete. In this paper, only results relating to autogenous shrinkage are presented. While shrinkage deformations were measured, cement hydration, pozzolanic reactions, and pore structure of concrete also were monitored to characterize the microstructural evolution of material. Very high autogenous shrinkage at an early age that stops 10 days after casting was observed. As far as we know, this sudden break in shrinkage kinetics has never been observed before in cement-based materials. The autogenous relative humidity measurements show high self-desiccation within the CRC. A relationship between autogenous shrinkage and self-desiccation of CRC is established and discussed.

Keywords: High-performance concrete; Hydration; Pore size distribution; Humidity; Shrinkage

During the last few years, very-high-strength concretes have been developed. Compact reinforced composite (CRC) elaborated by Aalborg Portland [1] is such a concrete. CRC is characterized by a high silica fume content (20–25% of cement weight), a very low water-to-cement (w/c) ratio (0.15–0.20), and a high compressive strength in the range from 150–400 MPa. Ductility of CRC is ensured by incorporation of steel fibers, typically 6% by volume. The dense microstructure of CRC gives it a superior durability compared to conventional high-strength concrete [2].

Control of these materials requires good knowledge of their mechanical properties. Also, the time-dependent phenomena have important roles for the structural engineer designing safe and serviceable structures. An experimental program was set up and several series of specimens were tested to study shrinkage and creep behavior of CRC with a water-to-binder ratio of 0.16. In this paper, results relating to autogenous shrinkage, cement hydration kinetics, and relative humidity change are presented. Thermogravimetric analysis (TGA) was used to investigate hydration reactions of cement and pozzolanic activity of silica fume particles. Pore structure of concrete was analyzed by mercury intrusion porosimetry at different ages of CRC. The relative humidity change within a sealed steel fiber-reinforced specimen was measured by a hygrothermal probe. The aim of these experiments was to improve the understanding of the original kinetics observed on autogenous shrinkage of CRC.

1. Experimental

1.1. Materials

The mix composition of the CRC is shown in Table 1. A white Portland cement containing 66.9% C_3S, 19.2% C_2S, 4.35% C_3A, and 1%C_4AF was used. The silica fume content was 24% based on the cement weight and the w/c ratio was typically 0.20. A dry superplasticizer of condensed napthalene sulfonate was used. The aggregate was quartzite sand with a maximum nominal size of 4 mm. The steel fibers, 12 mm long and 0.4 mm in diameter, were introduced into the mix at a volume of 6% to provide ductility in the structural behavior. CRC without fiber reinforcement (plain matrix) was cast with the same components without any change in the composition.

1.2. Mix

Cement, silica fume, sand, and dispersing powder agent were mixed in a 75-L laboratory mixer for 1 min before the addition of water and additional mixing for 3 min. For the plain matrix specimens, casting was carried out at the end of

* Corresponding author. Tel.: 33-2-40-37-16-67; Fax: 33-2-40-37-25-35; E-mail: ahmed.loukili@ec-nantes.fr.

0008-8846/99/$–see front matter
PII: S0008-8846(99)00022-8

Table 1
Steel fiber concrete mixture

Ingredient	Cement	Silica fume	Superplasticizer	Sand			Steel fibers	Water
				<0.25 mm	0.25 – 1 mm	1 – 4 mm		
Percent by mass	27.2	6.4	0.78	6.05	12.25	24.58	17.25	5.42

this mixing period. For the fiber-reinforced specimens, this was followed by the addition of steel fibers, after which all of the constituents were mixed for another 5 min to ensure a homogenous mix.

1.3. Samples and preparation of test specimens

The specimens used in this investigation were as follows:

- 110 × 220-mm cylindrical specimens to determine the compressive strength,
- 90 × 600-mm cylindrical specimens to measure autogenous shrinkage, and
- 90 × 180-mm cylindrical specimens for thermogravimetry, porosity tests, and to measure relative humidity within concrete.

All concrete specimens came from a single batch. They were cast in successive layers and compacted on a vibrating table. After casting, specimens were maintained at ambient temperature and saturated hygrometry during the setting process. All specimens were demoulded 22 h after mixing. To avoid desiccation , specimens 90 mm in diameter were immediately coated with epoxy resin and wrapped in aluminum sheet. The specimens were stored in a climate chamber with a controlled environment of 50% relative humidity and 20°C until the time of testing. Shrinkage strains are calculated from the relative deformation of two circular rings distant of 400 mm and fixed at equal distance from each end of the specimens to avoid side effects (Fig. 1). Three screws on spring maintain each ring fixed to the specimen. Three linear variable differential transformer (LVDT) sensors, distributed on three generating lines at 120°, measure the displacement between the two rings fixed to the concrete. A counterweight improved the verticalness of the sensor rod and the stability of the measurements. Thermocouple of type K was cast in the shrinkage specimens to control the concrete temperature from the start of tests. Deformation and temperature were recorded at 10-min intervals during the first 48 h and each hour afterwards.

Pore structure analysis was performed by mercury intrusion porosimetry on the hardened materials with a PoreSizer 9320 porosimeter (Micromeritics®). Because the maximum pressure applied is 200 MPa, pores are accessible where their diameters were in the range of 6 nm and 360 μm. The concrete fragments used for this investigation were taken from the core of sealed specimens (90 × 180-mm cylinders). They are immediately plunged in acetone for 6 h to stop the hydration of cement and then dried at 60°C for 12 h before being tested. A constant contact angle of 142° was used in the computations.

TGA combined with derivative thermogravimetric curve (DTG) was used to investigate the hydration of cement. This technique allows quantification of the free and bound water in concrete and contributes to the understanding of the cement hydration process. TGA was carried out using a TGS2 Thermobalance (Pekin Elmer). The samples, weighing approximately 50 mg, were heated from 20 to 1000°C under an argon flow at a heating rate of 10°C/min. The accuracy of the thermobalance weighing equipment was about 1 μg.

Autogenous relative humidity change was measured on a 90 × 180-mm specimen protected from environmental moisture exchange and stored at a constant temperature of 20 ± 1°C and relative humidity of 50 ± 5%. The measurement was made using a 5-mm diameter, Rotronic thermohygrometric probe (Vaisala), which is a convenient and accurate method for measuring relative humidity and temperature imposed by the concrete in the cavity during the test. During the casting, a wooden stick was placed in the middle of the cylindrical specimen (90 × 180 mm). At the 1-day age, the sample was demolded and immediately sealed, then the wooden stick was replaced by the probe. It is worth noting that the probe was previously calibrated with saturated salt solutions over the whole range of relative humidity. The experimental device was set up in a room at 20°C and 50% relative humidity. Data are logged continuously on the computer every 15 min for 3 months.

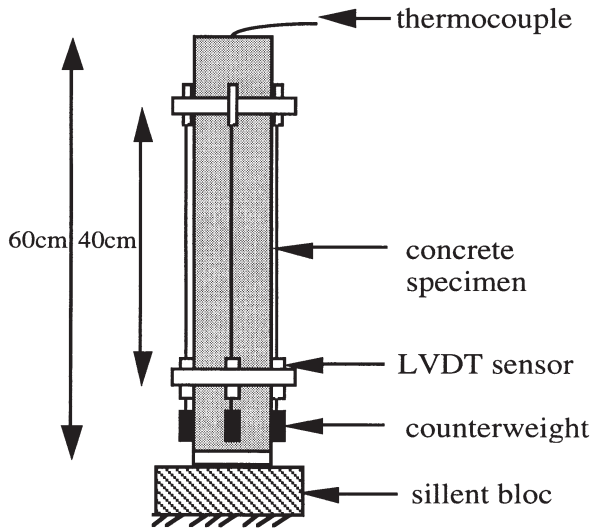

Fig. 1. Schematic diagram of the shrinkage frame.

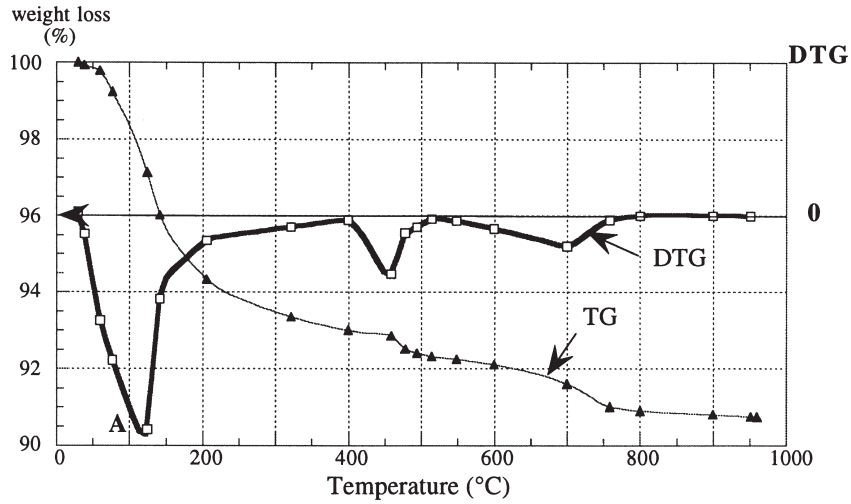

Fig. 2. Typical TG and DTG curves.

2. Test results and discussion

2.1. Cement hydration process

The hydration of cement was investigated by TGA. A typical curve is shown in Fig. 2. With respect to the tested samples taken from plain matrix specimens, point A (Fig. 2) is within a temperature range of 105–130°C. For comparative purposes the limit between free and bound water is defined at point A, in contrast to other authors who considered the limit close to 100°C [3] or 145°C [4]. A similar definition was used for analysis of reactive powder concrete [5].

The bound water quantity can be related to cement hydration by the classic Powers relation given in Eq. (1):

$$\alpha(\%) = \frac{W_{ne}(t)}{W_{ne}(t_\infty)} * 100 \quad (1)$$

where $W_{ne}(t)$ is the bound water content at time t, and $W_{ne}(t_\infty)$ is the water quantity necessary for complete cement hydration according to the calculation by Czernin [6]. For the cement used in this study, $W_{ne}(t_\infty) = 0.24$. Thermogravimetry also can be used to estimate the pozzolanic reaction of silica fume. The calcium hydroxide content is calculated from the DTG peak for temperatures between 420°C and 500°C. The peak between 600°C and 750°C represents the $CaCO_3$ decarbonation. A thorough description of the TGA and the calculation details were published previously [7].

The degree of hydration and the change of $Ca(OH)_2$ content at different ages are given in Fig. 3. The results show that the degree of cement hydration is very fast at an early age, but the evolution slows down after 4 days. At 28 days, the degree of hydration of cement is only 57.5%. Thus, nearly 377 kg/m^3 of unhydrated cement remains in the CRC. This significant amount of unreacted cement must be included in the granular skeleton of concrete and can take the place of ideal grains according to their intrinsic mechanical strength [8].

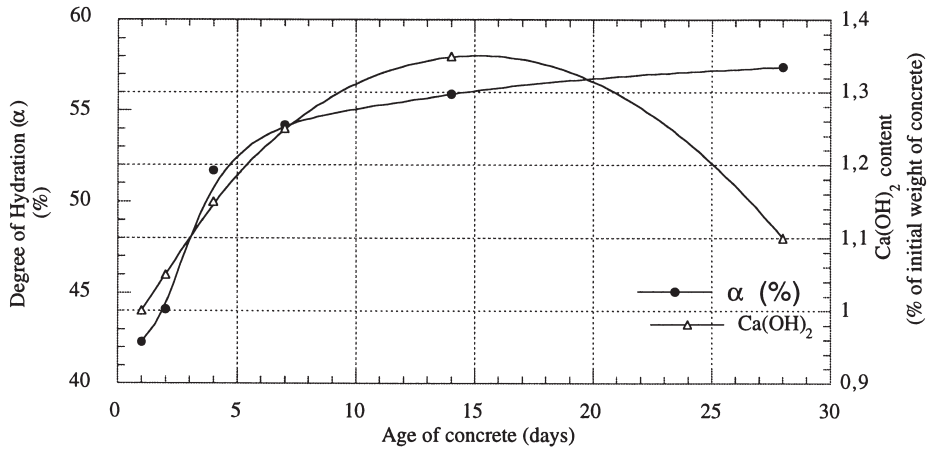

Fig. 3. Degree of hydration and $Ca(OH)_2$ content at different ages.

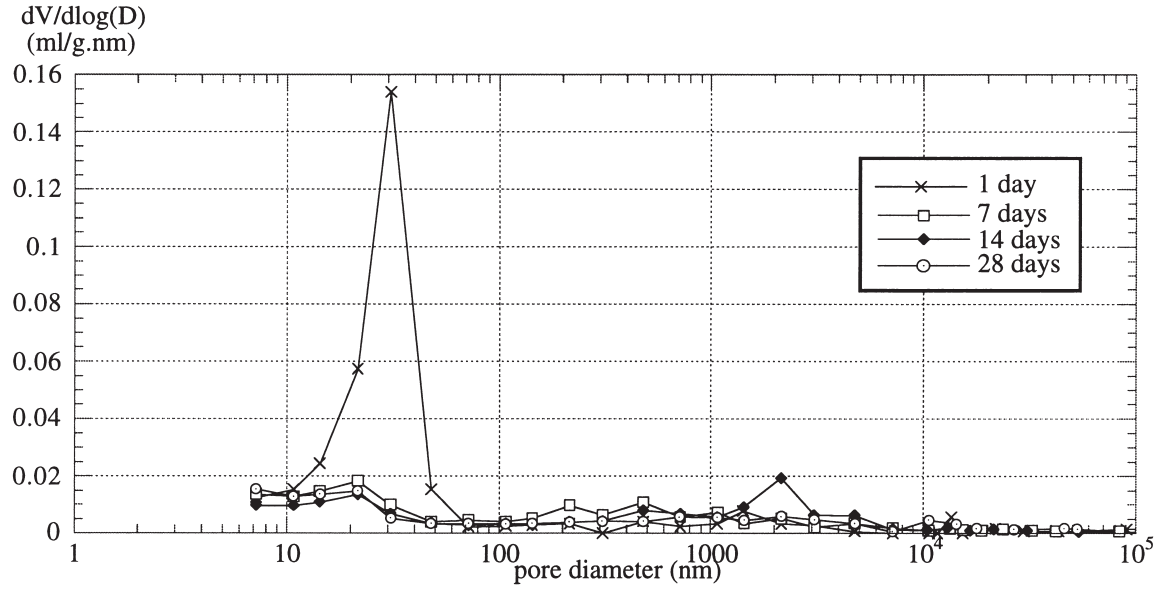

Fig. 4. Pore size distribution of the CRC at different ages.

Fig. 3 also shows that the $Ca(OH)_2$ content increases at an early age and reaches a maximum at about 14 days. Then, the calcium hydroxide content starts to decrease progressively. This illustrates well the competing reactions: cement hydration producing $Ca(OH)_2$ on the one hand and the pozzolanic reaction of the silica fume consuming calcium hydroxide on the other hand.

2.2. Pore structure analysis

It is considered that pores 6 nm or less in diameter correspond to gel pores that mainly exist in precipitated C-S-H structures. Pores between 6 to 50 nm in diameter correspond to capillary pores formed in hydrates, and those 50 nm or larger correspond to large-diameter capillary pores [9]. Pore size distributions of CRC at different ages are illustrated in Fig. 4.

It is shown that the porosity of CRC after only 24 hours is essentially constituted of pores formed in hydrates. A sharp main peak at about 30 nm is observed. This shows the absence of large capillary pores (diameter $>$50 nm) at an early stage after mixing. This result can be attributed to the higher silica fume dosage in the CRC (25% based on weight of cement). Accordingly, the higher fineness of silica fume particles allows efficient filling of the voids between cement particles in fresh concrete. During the first week, we observed a significant decrease in pore volume (87%) corresponding to the peak 30-nm pore diameter and a displacement of this peak towards the pores of about 20-nm diameter. This change in pore size distribution was certainly due to pozzolanic reaction that occurs between the microsilica and the calcium hydroxide to form more C-S-H gel. This led to the refininement and densification of porous structure of concrete. Fig. 4 also shows that after 7 days, there was no significant change in pore structure. Some macroscopic pores peaks between 2 and 10 μm can be observed. It is possible that the structure of capillary pores was modified by the microcracking generated by the heat treating of sample before the mercury porosimetry test.

It is important to note that a significant porosity for pores smaller than 6 nm in diameter (gel pore) is invisible by mercury intrusion porosimetry. Accordingly, quantitative analysis of the total pore volume for pore radii larger than 0.14 nm can be obtained by helium picnometry. The apparatus used for this analysis is an Accupic 1330 (Micromeritics), with an accuracy of 0.01%. The volume of the tested specimen was about 100 mm^3. From the material density d_{Hg} and porosity n_{Hg} measured by mercury intrusion porosimetry for pore size larger than 6 nm, the total porosity higher than 0.14 nm can be deduced by using the total density obtained with helium picnometry d_{He} given in Eq. (2):

$$n_{He} = 1 - (d_{Hg}/d_{He}). \quad (2)$$

The porosity relative to the pores less than 6 mm in size was 27% at the age of 7 days, 30% at the age of 14 days, and 41% at the age of 28 days. This quantitative result shows the higher fineness of the porous network giving a compact microstructure of concrete from an early age. On the other hand, one can note limits of mercury intrusion porosimetry to characterize the pore structure of materials with very low w/c ratios.

2.3. Autogenous shrinkage

Fig. 5 presents the autogenous shrinkage measured on two specimens of plain and fiber-reinforced matrices.

For both concretes, shrinkage is characterized by very rapid kinetics at an early age. At the 1-day age, the deforma-

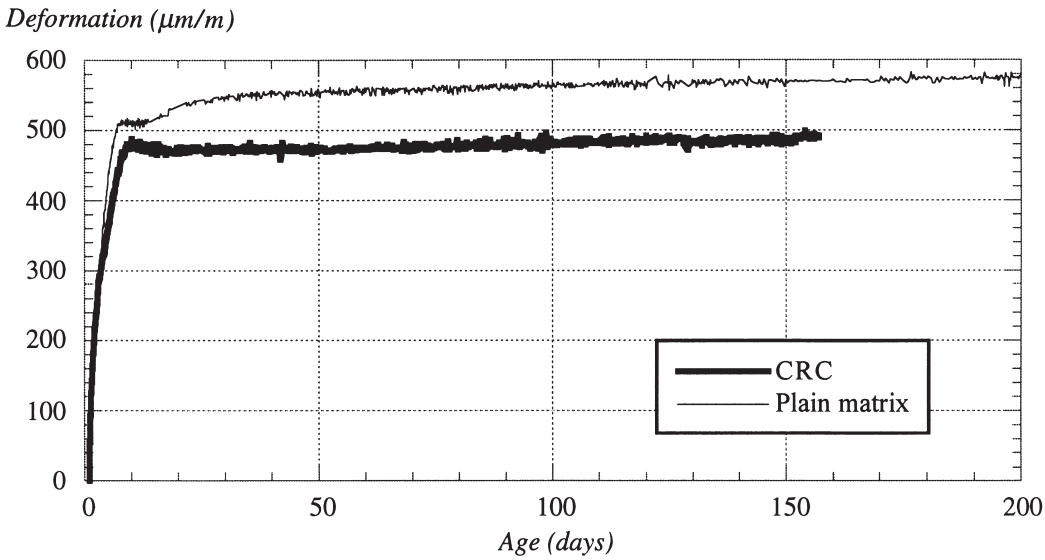

Fig. 5. Autogenous shrinkage of plain and steel fiber-reinforced specimens.

tion rate reached 45% of the final deformation (measured value at 160 days) and 95% after only 10 days. Beyond this date the autogenous shrinkage of CRC remained practically constant while shrinkage of the plain matrix developed very slowly (1 μm/m per day). The recorded deformation between 10 and 160 days is about 20 μm/m for CRC and 60 μm/m for plain matrix.

The curve of the CRC shrinkage presents an originality in comparison with the normal or high-strength concrete with or without fibers. A sudden change is noted in shrinkage kinetics 10 days after water addition. As far as we know, this phenomenon never before had been so clearly observed in cement-based materials. Nevertheless, a difference can be noted in the behavior between both concretes. At the age of 7 days, the shrinkage of the plain matrix is completely stopped for 4 days (Fig. 5). Then, its evolution is less pronounced than that recorded during the first week. This phenomenon cannot be due to an experimental artifact, as it is observed on both specimens used for the measurements [7]. In our opinion, it can only be the consequence of a mechanical effect: during the first week, the high shrinkage strains lead to internal stresses in paste as well as in aggregates. If the viscoelastic character of the paste is excluded, these stresses would be proportional to macroscopic shrinkage strains. The level observed on the curve of plain matrix specimen might correspond to the time when the stresses exceed ultimate tensile strength in cement paste. This state causes multicracking in the concrete. In the CRC, these microcracks are bridged by steel fibers that allow resumption of the tensile stresses. In the plain matrix the microcracking leads to relaxation of the specimen and the shrinkage will resume in the matrix.

As for the sudden break in shrinkage kinetics at the 10-day age, it is observed on the CRC as well as on the plain matrix specimens; therefore, this phenomenon cannot be related to the presence of fibers, which can make the material very rigid when they are solicited. TGA tests showed that cement hydration is significantly slowed after a 1-week hardening because of a scarcity of free water, but it does not stop completely. Thus, the stoppage of shrinkage can hardly be attributed to an interruption of the hydration process in the CRC. To know the origin of this phenomenon, it is necessary to study the influence of other parameters that have an influence on autogenous shrinkage, e.g., the aggregate content (48% by volume in CRC). This hypothesis was investigated by measurement of autogenous shrinkage on a plain matrix specimen without aggregates (cement paste). This is the best test to check if the aggregates can restrain the shrinkage in the CRC so as to stop it completely. The w/c and silica fume-to-cement ratios of the cement paste were kept at about 0.20 and 0.24, respectively. Fig. 6 shows that the sudden break also was found on the shrinkage curve of the cement paste specimen at the 10-day age. It can be concluded that neither fibers nor aggregates are involved in the halting of CRC autogenous deformation 10 days after water addition; therefore, this phenomenon seems to originate within cement paste where the binder chemistry controls the shrinkage mechanism of CRC. For better analysis of this phenomenon, it would be very instructive to follow the self-desiccation evolution within the CRC.

2.4. Self-desiccation measurements within the CRC

For better estimation of the relative humidity change in CRC, a second measurement was done on a classic mortar with w/c ratio of 0.42. Fig. 7 shows that the CRC undergoes very high self-desiccation in comparison with the classic mortar, which certainly was due to the low w/c ratio [10] as well as to high silica fume dosage in CRC [11].

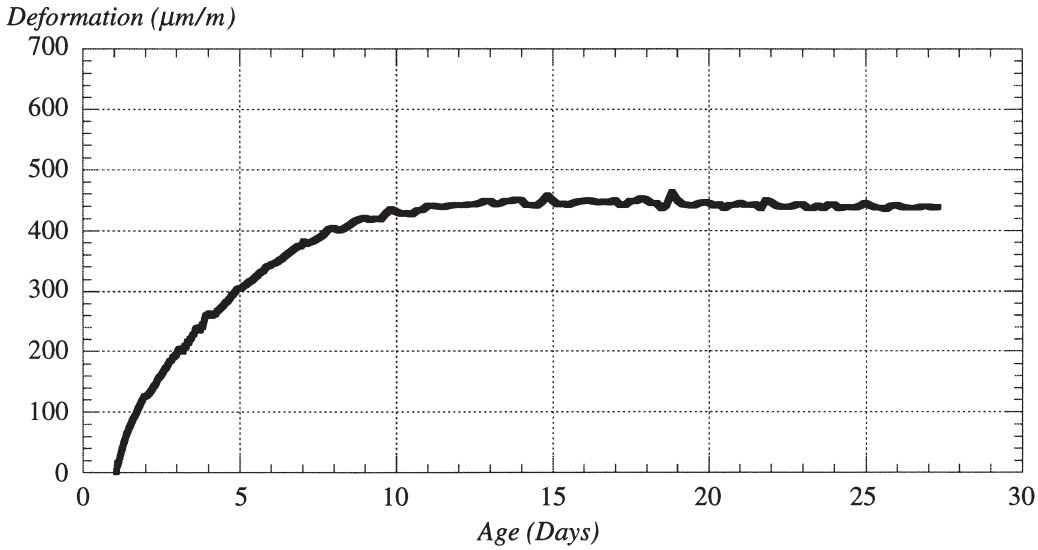

Fig. 6. Autogenous shrinkage of cement paste specimen.

It can be observed that the lowering of relative humidity in CRC is very rapid at short times. At 8 days, the internal relative humidity reaches 73%, then it decreases very slowly and reaches 68% after 3 months. At this time, the relative humidity within classic mortar is only 91%. In comparison, in a high-performance concrete with w/c ratio of 0.27 and containing 10% silica fume, the relative humidity is 68% after 1 year's measurements [8].

Fig. 8. show the evolution of autogenous shrinkage and relative humidity within the CRC. The rapid evolution stage of autogenous shrinkage (during the first week) corresponds to the time when self-desiccation is intense in the material. Fig. 8 also shows clearly that autogenous shrinkage stops (point A) when internal relative humidity reaches 73% (point B).

Based on data reported in the literature and experimental results of this study, we suggest an explanation for the particular kinetics of CRC autogenous shrinkage. Fig. 9 illustrates the relationship between relative humidity change and autogenous shrinkage.

Apart from part OA where the relative humidity is higher than 96% (the probe is inaccurate in this field), the curve shows three parts where the shrinkage varies linearly according to relative humidity: AB, BC, and CD. The first part (AB) ranging from 76–96% corresponds to the moment when the hydration reactions are intense within the material.

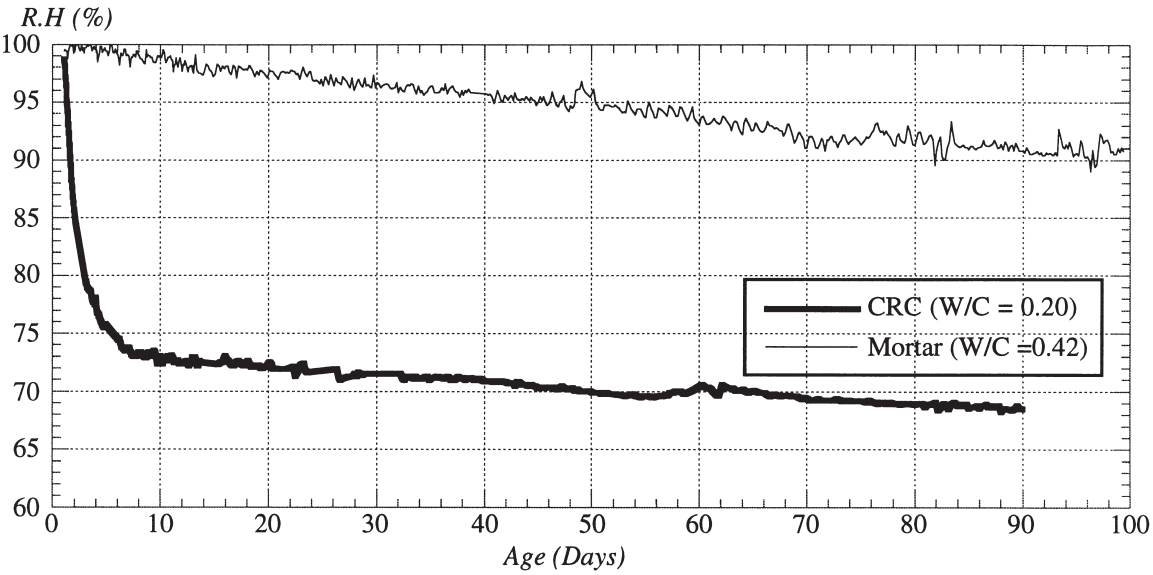

Fig. 7. Autogenous relative humidity change of concretes with different w/c ratios.

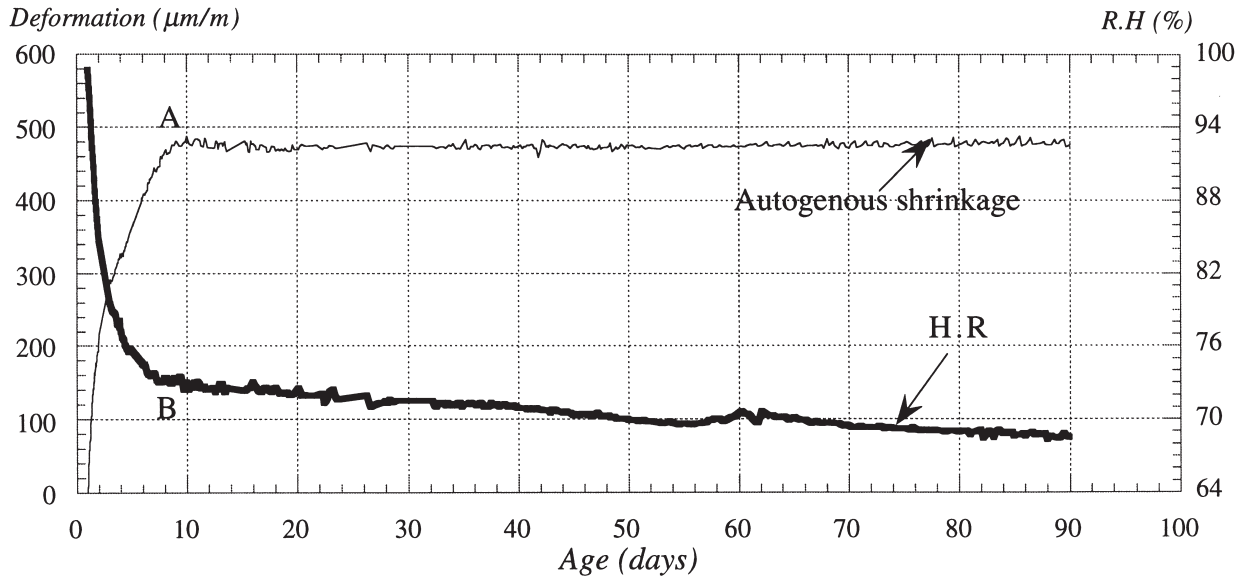

Fig. 8. Evolution of autogenous shrinkage and relative humidity within the CRC.

This might be due to the rapid consumption of free water for cement hydration as well as the high dosage of silica fume in the CRC. This led to a finer pore structure from the first week as shown by mercury porosimetry tests (Fig. 4). The capillary tensions are important and increase the skeleton contraction and self-desiccation within CRC, as was experimentally observed (Fig. 5). Therefore, the rapid development of autogenous deformation at an early age is a direct consequence of this self-desiccation. The curve then records a slight change of slope (part BC) between 73–76% for a period of 5 days. During this period, the shrinkage speed is less important because of a depletion of the hydration water in CRC. When relative humidity reaches 73% a large increase of slope can be observed. This corresponds to the beginning of stabilization of the relative humidity in the concrete and thereby the autogenous shrinkage. Below 73% (CD), the humidity lowering in the material may not be due to the free water diminution in the capillary pores but may be essentially due to the consumption of the hydrates adsorbed water [8]. Therefore, cement hydration is considerably hindered but not completely stopped. This supposition was supported by TGA, which showed very low hydration kinetics after 1 week (Fig. 3). It is significant to note that the intense self-desiccation within CRC does not prevent the pozzolanic activity of silica fume. It can be deduced that the pozzolonic reaction does not use evaporable water. This result is in very good agreement with the findings of Sellevold and Justens [12]. Therefore, the significant amount of

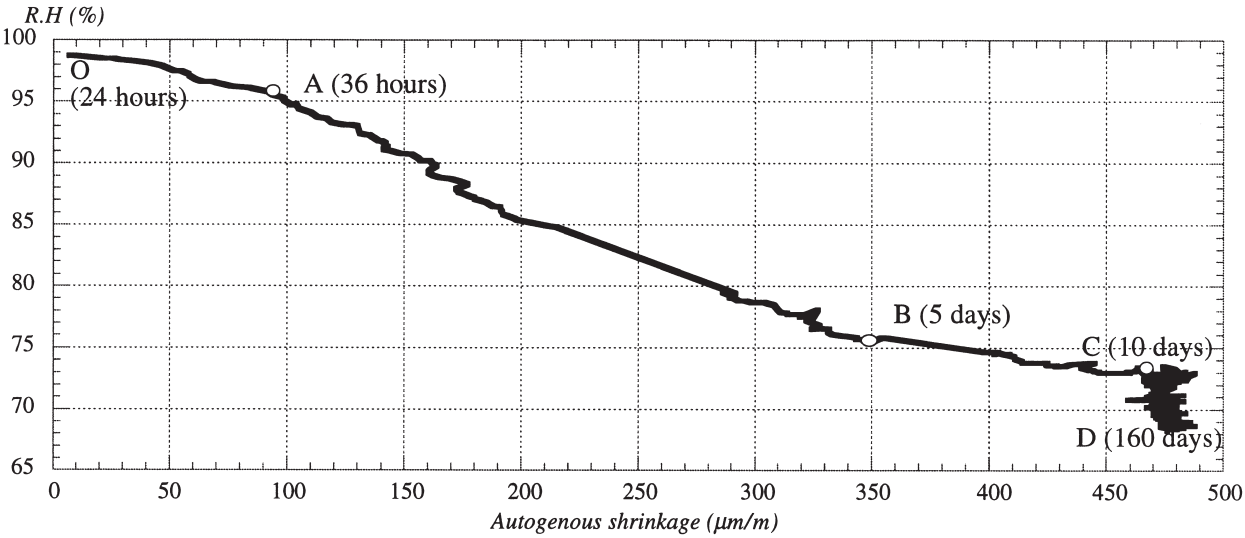

Fig. 9. Relationship between autogenous shrinkage and relative humidity within the CRC.

unreacted cement (about 48% of the initial mass of cement at 7 days) may reinforce the granular skeleton of concrete, which leads to a stiffening effect. It can be concluded that this phenomenon, coupled with the lack of evaporable water, hampers considerably the autogenous deformation that becomes not easily perceptible 10 days after casting.

3. Conclusions

Results presented in this work showed that cement hydration in CRC is incomplete because of its low w/c ratio. The pozzolanic activity of the silica fume becomes predominant 2 weeks after mixing despite the very low relative humidity within the material at this age. Mercury intrusion porosimetry completed by helium picnometry showed an extremely low porosity, especially after 1 week of hardening. A high autogenous shrinkage in an early age, which practically finished 10 days after batching, was observed. Various experiments, particularly the relative humidity change within CRC, suggest an explanation for this phenomenon. It can be attributed to the high self-desiccation at an early age due to both a very low w/c ratio and a high silica fume content. The granular skeleton is reinforced by unreacted cement and thereby hinders considerably autogenous shrinkage.

References

[1] H.H. Bache, Compact reinforced composite, basic principles. CBL Report 41, Aalborg Portland, 1987, p. 87.
[2] M.C. Andrade, M. Frias, B. Aarup, Durability of ultra high strength concrete: compact reinforced composite, in: F. de Larrard (Ed.), 4th International Symposium on Utilization of High-Strength/High-Performance Concrete, ENPC Press, Paris, 1996, pp. 529–534.
[3] B. El-jazairi, J.M. Illston, Cem Concr Res 7 (1977) 247–258.
[4] H.F.W. Taylor, Cement Chemistry, Academic Press Limited, London, 1990.
[5] M. Cheyrezy, V. Maret, L. Frouin, Annales de l'Institut Technique du Bâtiment et des Travaux Publics, No. 532, 1995, pp. 103–111.
[6] B. Czernin, Cementkemi för Byggare, Svesnka Cement Föreningen, 1956.
[7] A. Loukili , Ph.D. Thesis, Ecole Centrale de Nantes, Nantes, 1996.
[8] V. Baroghel-Bouny, Ph.D. Thesis, Ecole Nationale des Ponts et chaussées, Paris, 1994.
[9] H. Uchikawa, S. Hanehara, H. Hiaro, Cem Concr Res 26 (6) (1996) 101–111.
[10] M. Buil, Research Report LPC, No. 92, 1979.
[11] O. Mejlhede Jensen, P. Freiesleben Hansen, ACI Mater J 93 (6) (1996) 539–543.
[12] E.J. Sellevold, H. Justens, Fourth International Conference, ACI, SP-132, Istanbul, 1992, pp. 891–902.